Sensors and Actuators B 228 (2016) 134–143

Contents lists available at ScienceDirect

Sensors and Actuators B: Chemical

journal homepage: www.elsevier.com/locate/snb

Sulfonated graphene anchored with tin oxide nanoparticles for detection of nitrogen dioxide at room temperature with enhanced sensing performances

Sen Liu [a], Ziying Wang [a], Yong Zhang [a], Jiacheng Li [a], Tong Zhang [a,b,*]

[a] State Key Laboratory on Integrated Optoelectronics, College of Electronic Science and Engineering, Jilin University, Changchun 130012, PR China
[b] State Key Laboratory of Transducer Technology, Chinese Academy of Sciences, PR China

ARTICLE INFO

Article history:
Received 27 June 2015
Received in revised form 1 December 2015
Accepted 7 January 2016
Available online 11 January 2016

Keywords:
Sulfonated graphene
NO_2 sensing
Room temperature
SnO_2 nanoparticle

ABSTRACT

The development of graphene-based room temperature gas sensors has drawn massive attention due to their unique advantage of gas sensing at room temperature. In this paper, in pursuit of developing high-performance graphene-based gas sensors, a NO_2 gas sensor has been successfully fabricated using sulfonated reduced graphene oxide (S-rGO) anchoring with SnO_2 nanoparticles as sensing materials. The SnO_2 nanoparticles modified S-rGO (SnO_2/S-rGO) hybrids were prepared by deposition of SnO_2 nanoparticles on the surface of S-rGO through hydrothermal synthesis method. The combined characterizations of X-ray diffraction, UV–vis spectroscopy, X-ray photoelectron spectroscopy, transmission electron microscopy, energy-dispersive spectroscopy, as well as N_2 sorption isotherm indicate the successful preparation of SnO_2/S-rGO hybrids with porous structure. Most importantly, SnO_2/S-rGO hybrids exhibit good sensing performances for detection of NO_2 at room temperature, such as high response, fast response and recovery rate, and good selectivity. The sensor based on SnO_2/S-rGO hybrids exhibits better sensing performances than the previously reported rGO-based gas sensors. Furthermore, the excellent sensing performances of sensor based on SnO_2/S-rGO also render it suitable for development of high performance gas sensors operated at room temperature.

1. Introduction

Since the first discovered in 2004, graphene has been attracted considerable attention due to its excellent chemical and physical properties, which ensure its wide applications in the fields of energy conversion and storage, adsorption and separation, catalysis, sensing, electronic devices, and so on [1–4]. Particularly, graphene has been proven as an exciting candidate as active constituent for fabrication of high-performance chemiresistor gas sensors [5–7]. Taking advantages of excellent sensing performances of conventional metal oxides, much effort has been paid on developing gas sensors using graphene-metal oxide hybrids as sensing materials. Recent studies have shown that introduction of graphene into metal oxide matrix dramatically enhances the sensing performances, compared to the sensors based on pure metal oxides. For example, graphene-SnO_2 nanorods [8], hierarchical SnO_2@reduced graphene oxide (rGO) [9], SnO_2 nanofibers-rGO [10], and WO_3 nanorods/graphene [11] have been successfully constructed and used for detection of gases (such as ethanol, NO_2, acetone and hydrogen sulfide) with enhanced sensing performances. However, relatively high temperature (>100 °C) is required for detection of gases using above mentioned graphene-based materials, resulting in the shortcomings of high power consumption, poor stability, impeding their further applications.

Alternatively, graphene also exhibits other excellent properties, such as high carrier mobility at room temperature and detectable change in its resistance after adsorption or desorption of gas molecules, providing a promising sensing material for fabrication of room temperature gas sensors [12]. It is reported that pure graphene materials prepared by various methods, such as chemical vapor deposition [13], rGO obtained by heat reduction method [14,15], and chemical reduction method [16] have been used for detection of NO_2 as room temperature. However, the above graphene-based sensors exhibit obvious disadvantages of weak response, long response time and recovery time, which has unfortunately limited their large-scale practical applications. Therefore, much attention has been focused on developing graphene-based

* Corresponding author.
E-mail address: zhangtong@jlu.edu.cn (T. Zhang).

http://dx.doi.org/10.1016/j.snb.2016.01.023
0925-4005/

gas sensors with excellent sensing performances for detection of gases operated at room temperature.

Efforts at improving sensing performances of graphene-based gas sensors have centered primarily two approaches to enhance transduce efficiency from target gas to electric signal. One involves rational design of sensor with new structure to match the properties of sensing materials. The second involves optimizing semiconductor properties of sensing materials by fine-tune chemical affinity between target gas and sensing materials. Notably, tailoring semiconductor properties of graphene-based sensing materials should be a promising method for enhancing sensing performances. Recently, researchers have attempted to fine-tune the semiconductor properties of graphene by modification of graphene with other functional hybrids to overcome shortcomings of graphene-based room temperature gas sensors. For instance, Chung and co-authors have fabricated gas sensors based on Pd nanocube–graphene hybrids for detection of H_2 [17]; Yang et al. [18]; have constructed sensor using porous poly(3,4-ethylenedioxythiophene) (PEDOT) modified rGO hybrids as sensing materials for detection of NO_2 Russo et al. [19]; have developed sensors based on rGO-SnO_2-Pt hybrids for H_2 sensing at room temperature; Li et al. [20] have fabricated SnO_2-rGO hybrids-based sensors for detection of NH_3 at room temperature. Furthermore, Cu_xO nanoflower/graphene composites [21], Co_3O_4-intercalated rGO [22], ZnO–graphene hybrids [23,24], SnO_2/rGO hybrids [25], as well as SnO_2-rGO-carbon nanotubes hybrids [26] have also been used for detection of NO_2 at room temperature.

It is obviously seen that sensing performances of graphene-based gas sensors have been tremendously enhanced by modification of graphene with metal oxides. For example, such graphene-based sensors could recovery to the initial resistance by returning the sensors into air without heating, or ultraviolet light. Additionally, the response time and recovery time of the sensors are also decreased from several minute down to tens of second. However, the sensing performances should be further enhanced for their potential applications, especially in specific environmental.

More recently, Shi and co-authors have reported fabrication of graphene-based gas sensor using sulfonated rGO (S-rGO) as sensing materials for NO_2 sensing at room temperature. The results show that the sensitivity of the sensors increased by modified rGO with sulfonic acid group [27]. Unfortunately, the response time and recovery time are still long (more than several minute). This is mainly ascribed to inherent affinity between target molecule (NO_2) and sensing material (S-rGO). Although sulfonic acid group has been introduced into rGO materials, the response to NO_2 may be still performed by interactions between NO_2 and active sites in S-rGO (defects and graphitic structure), which is similar with the sensing mechanism for NO_2 detection based on rGO-based gas sensors [16].

Inspired by the aforementioned concepts, we have undertaken to modify S-rGO with SnO_2 nanoparticles for tuning the properties of S-rGO to improve the sensing performances. The SnO_2 nanoparticles modified S-rGO (SnO_2/S-rGO) hybrids were prepared by deposition of SnO_2 nanoparticles on S-rGO by the hydrothermal synthesis method. By introduction of SnO_2 nanoparticles, SnO_2/S-rGO hybrids exhibit high sensitivity and fast response-recovery characteristic to NO_2 at room temperature.

2. Experimental

2.1. Preparation of S-rGO

GO was prepared by the modified Hummers method according to previously reported publication [28].

The S-rGO was prepared according to previous publication using GO as precursor [29]. In a typical synthesis of S-rGO, pH value of GO aqueous dispersion (7.5 mL, 1 mg/mL) was adjusted to 9–10 with sodium carbonate solution (5 wt%), followed by addition of sodium borohydride ($NaBH_4$) solution (60 mg of $NaBH_4$ dissolved into 1.5 mL of water). After that, partially reduced graphene oxide (P-rGO) was obtained by heating the above mixture at 80 °C for 1 h under stirring. P-rGO was centrifuged and rinsed with water several times, and then re-dispersed in 7.5 mL of water for further use. The aryl diazonium salt used for sulfonation was prepared by the reaction of sulfanilic acid (9.2 mg) and sodium nitrite (3.6 mg) in 20 mL of HCl solution (0.05 M) in an ice bath. The solution of diazonium salt was added into P-rGO dispersion in an ice bath for 2 h. Sulfonated P-rGO was obtained by centrifugation and rinsing with water for several times, and re-dispersed in 7.5 mL of water. Finally, 2.5 μL of hydrazine hydrate was added into sulfonated P-rGO dispersion, followed by heating at 100 °C for 1 h under stirring. The S-rGO was obtained by centrifugation and rinsing with water for several times, and re-dispersed in 7.5 mL of water.

2.2. Preparation of SnO_2/S-rGO hybrids

SnO_2/S-rGO hybrids were prepared by deposition of SnO_2 nanoparticles on the surface of S-rGO through hydrothermal synthesis method. In a typical synthesis, 24 mg of $SnCl_4$ was added into 20 mL of H_2O, followed by addition of 1 mL of S-rGO dispersion. After sonication for 10 min, the mixture was transferred into a 50 mL Teflon-lined stainless steel autoclave and then heated at 180 °C for 12 h. After that, the products were collected by centrifugation, washing by water, and dispersed into water for characterization and further use.

2.3. Characterizations

UV-vis spectra were obtained on a UV-2450 Spectrophotometer. Powder X-ray diffraction (XRD) datum was recorded on a RigakuD/MAX 2550 diffractometer with Cu Kα radiation (λ = 1.5418 Å). X-ray photoelectron spectroscopy (XPS) analysis was measured on an ESCALAB MK II X-ray photoelectron spectrometer using Mg as the exciting source. Transmission electron microscopy (TEM) measurement was made on a HITACHI H-8100 electron microscopy (Hitachi, Tokyo, Japan) with an accelerating voltage of 200 kV. Nitrogen sorption isotherm was obtained at −196 °C with a JW-BK 132F analyzer. Samples were prepared for measurement by treating at 150 °C under nitrogen atmosphere for 12 h. Pore size distribution was calculated using Barrett–Joyner–Halenda (BJH) method. The chemical composition mapping through energy-dispersive spectroscopy (EDS) of the sample was examined by field emission scanning electron microscopy (JSM-6700F). A PerkinElmer TGA 7 unit was used to carry out the thermogravimetric analysis (TGA) in air at a heating rate of 10 °C/min. Raman spectra were obtained on J-YT64000 Ramanspectrometer with 514.5 nm wavelength incident laser light.

2.4. Fabrication of gas sensors

The sensors were fabricated by dropping SnO_2/S-rGO dispersion onto the ceramic substrate. Before dropping the sensing materials, two pairs of Au electrodes were printed on one side of ceramic substrate as signal electrode and another side of ceramic substrate as heating electrode. During the process for gas sensing, the temperature of sensors was fixed at 30 °C by heating ceramic substrate. For dropping sensing materials onto electrode, 0.3 μL of SnO_2/S-rGO aqueous dispersion was dropped on the surface of signal electrode, followed by dryness at room temperature.

Gas sensing properties were examined using a static test system by CGS-8 intelligent test meter (Beijing Elite Tech. Co., Ltd., China). Target gas with various concentrations was prepared by injection of various volume of NO_2 gas with fixed concentration into a test chamber (about 1 L in volume). After fully mixed with air (relative humidity was about 25%), the sensor was put into the test chamber. When the resistance of sensor reached a constant value, the sensor was taken out to recover in air. The response of the sensor was defined as $S = (R_a - R_g)/R_g$Í100, where R_a is the resistance of the sensor in air and R_g is the resistance of the sensor in target gas reaching a stable value. The 100% response signal is defined as the R_g changed from R_a to the stable value when the sensor was putted in the target gas. In this work, the response time is defined as the time required until 90% of the response signal is reached, while the recovery time denotes the time needed until 90% of the original baseline signal is recovered.

3. Results and discussion

It is well known that the modification of rGO with metal oxides could improve the sensing performances of graphene-based gas sensors [30,31]. To enhance the sensing performances, S-rGO was modified with SnO_2 nanoparticles by hydrothermal synthesis method. During the hydrothermal synthesis, $SnCl_4$ conversed into SnO_2 nanoparticles deposition on the surface of S-rGO, where the defect of S-rGO exhibits as template for formation of SnO_2 nanoparticles. The scheme illustrating the synthetic process of SnO_2/S-rGO hybrids is shown in Fig. 1.

In this work, S-rGO was prepared by covalent modification method, which has been proven as an effective method for introduction of sulfonic acid group onto rGO [32,33]. Thus, formation of S-rGO from GO is simply characterized by UV–vis spectroscopy and XPS analysis. Fig. 2 shows UV–vis spectra of GO and S-rGO thus obtained. It is seen that GO exhibits a strong absorption peak at 230 nm and a broad peak at 300 nm, which are corresponding to $\pi \rightarrow \pi^*$ transitions of aromatic C=C band and $n \rightarrow \pi^*$ transitions of C=O band in GO, indicating the successful preparation of GO from graphite [32]. Additionally, S-rGO shows a strong absorption peak at 272 nm, indicating the reduction of GO by hydrazine hydrate [34]. Furthermore, a well-dispersed S-rGO aqueous dispersion is obtained by sonication of S-rGO in water, which is different from rGO prepared by reduction of GO using hydrazine as reducing agent in the absence of stabilizing agent. The good dispersing ability of S-rGO is attributed to the modification of rGO with water-soluble sulfonic acid, further confirming the formation of S-rGO.

The reduction of GO during preparation of S-rGO was further confirmed by XPS characterization. Fig. 3a shows XPS profile of C1s for SnO_2/S-rGO hybrids. It is seen that C1s spectrum could be deconvoluted into three peaks at 284.6 eV, 286.6 eV, and 288.9 eV, associated with C—C, C—O, and C=O bands, respectively [35]. It is noted that the intensities of C—O, and C=O bands are much lower than that of C-C band, compared to GO used as precursor for preparation of S-rGO. Furthermore, the ratio of C—O and C=O in the carbon-based bands is also much lower than that of rGO obtained by the chemical reduction of GO [35]. Fig. 3b shows the Sn3d spectrum of SnO_2/S-rGO hybrids. The hybrids show two bands centered at 487.3 eV and 495.8 eV, which are associated with $Sn3d_{5/2}$ and $Sn3d_{3/2}$, indicating the formation of SnO_2 in the hybrids. Additionally, the O1s spectrum of SnO_2/S-rGO hybrids is also examined, as shown in Fig. 3c. Two bands centered at 533.3 eV and 532.2 eV are observed, which are attributed to the C-O band and C=O band in S-rGO. A new peak at 531.5 eV associated with Sn—O band is also observed in SnO_2/S-rGO hybrids.

Based on the results of XPS spectra, the composition of SnO_2/S-rGO hybrids is C 8.9%, O 64.84%, S 0.56%, and Sn 25.71%. It is seen that the ratio of O/Sn is 2.52, which is higher than that of SnO_2, attributed to the presence of O-containing groups in S-rGO. To accurately examine the content of S-rGO in the SnO_2/S-rGO hybrids, the sample was characterized by TGA. Fig. S1 shows the TG curve of SnO_2/S-rGO hybrids, indicating the content of S-rGO in the final hybrids is 4.38%, which is attributed to the weight loss in TG curve with temperature ranging from 200 to 600 °C.

To tune semiconductor properties of S-rGO for improvement of sensing performances, S-rGO was modified with SnO_2 nanoparticles by the hydrothermal method. Fig. 4 shows XRD pattern of the samples obtained by hydrothermal treatment of $SnCl_4$ in the presence of S-rGO. The sample exhibits eight peaks at 2θ of 26.57, 33.70, 37.77, 51.81, 62.40, 65.47, 71.50 and 78.05°, which are attributed to the (1 1 0), (1 0 1), (2 0 0), (2 1 1), (3 1 0), (3 0 1), (2 0 2) and (3 2 1) planes of tetragonal rutile SnO_2 (JCPDS File no. 41–1445), indicating formation of SnO_2 crystals [36]. Furthermore, no peak associated with S-rGO is observed for the samples, which may be attributed to the low content of S-rGO in the final hybrids. The XRD pattern exhibits relatively wide diffraction peaks, suggesting formation of SnO_2 nanoparticles with relatively small size. Furthermore, the particle size of SnO_2 nanoparticles was also calculated using the Scherrer's equation. The Scherrer's equation is as follows: $D = 0.89\lambda/\beta\cos\theta$, where D is the average diameter of the crystallite, λ (Cu Kα) = 1.5418 Å and β is the full-width at half-maximum of the diffraction lines [37,38]. The average size of SnO_2 nanoparticles in SnO_2/S-rGO hybrids is 7.5 nm, 6.09 nm, 3.67 nm, and 3.77 nm, according to the diffraction peak of (1 1 0), (1 0 1), (2 1 1) and (3 0 1).

The formation of SnO_2/S-rGO hybrids was further confirmed by the Raman spectra. Fig. S2 shows the Raman spectra of S-rGO, SnO_2/S-rGO hybrids and SnO_2 nanoparticles. Two strong bands centered at 1350 cm^{-1} and 1600 cm^{-1} are observed for S-rGO and SnO_2/S-rGO hybrids, which are attributed to the D band and G band in rGO-based materials, indicating the formation of rGO-based materials. Furthermore, SnO_2 nanoparticles exhibit two obvious bands at 569 cm^{-1} and 1147 cm^{-1} associated with SnO_2 crystals. Notably, SnO_2/S-rGO hybrids also show two weak bands at 569 cm^{-1} and 1147 cm^{-1}, indicating the formation of SnO_2/S-rGO hybrids.

The composition of SnO_2/S-rGO hybrids was further characterized by the EDS mapping to probe the elements' location. As shown in Fig. 5a–e, SnO_2/S-rGO hybrids are composited by C, O, S, and Sn elements distributing the whole samples. Furthermore, the corresponding EDS spectrum (Fig. 5f) also indicates that the samples are comprised of C, O, S, and Sn elements. The peak attributed to Si is also observed, which is associated with the substrate used for EDS characterization.

The structure of SnO_2/S-rGO hybrids was further examined by TEM images. Fig. 6a shows low magnification TEM image of SnO_2/S-rGO hybrids. It is seen that the sample shows typical flake-like morphology with the size about several micrometer, in agreement with the unique two-dimensional layer structure of rGO-based materials, indicating the formation of graphene-based materials. Additionally, unlike the smooth surface of rGO, numerous nanoparticles are observed on the surface of graphene-based materials for SnO_2/S-rGO hybrids, as shown in Fig. 6b. A higher magnification TEM image (Fig. 6c) further confirms the formation of SnO_2 nanoparticles on the surface of S-rGO. Fig. 6d shows the high resolution TEM image (HR-TEM) of SnO_2 nanoparticles on S-rGO layer. Based on the HR-TEM image, the particles size of SnO_2 nanoparticles is about 5–7 nm, which is agreement with the particle size obtained by Scherrer's equation from XRD pattern. Furthermore, it is obviously seen that lattice fringe of each SnO_2 nanoparticle can be clearly observed, indicating the formation of SnO_2 with high crystallinity.

It is deduced that modification of S-rGO with SnO_2 nanoaprticles could prevent agglomerate of S-rGO affecting by the π–π

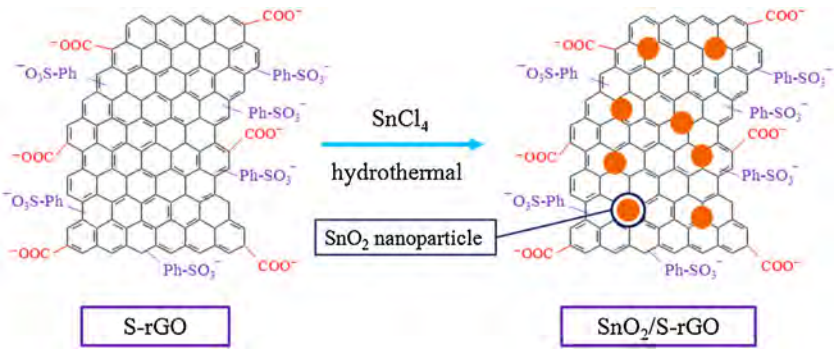

Fig. 1. A scheme to illustrate the modification of S-rGO with SnO_2 nanoparticles by hydrothermal synthesis method.

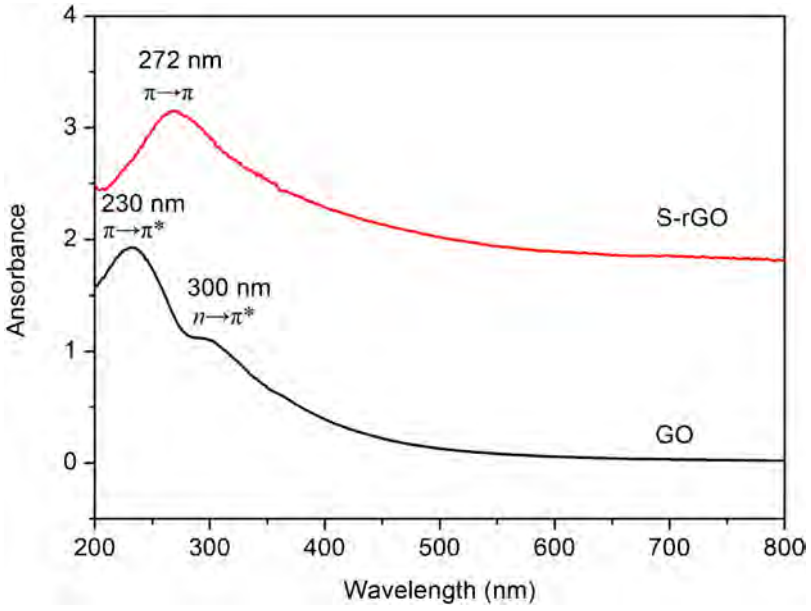

Fig. 2. UV–vis spectra of GO and S-rGO.

interaction between them, leading to the formation of porous structure. Thus, the porous structure of SnO_2/S-rGO hybrids was characterized by the N_2 sorption isotherms. Fig. 7 shows N_2 adsorption/desorption isotherm of SnO_2/S-rGO hybrids. It is seen that the N_2 amount adsorbed by hybrids increases with increasing the relative pressure, indicating the formation of porous structure. The inset of Fig. 7 shows the corresponding pore size distribution curve of SnO_2/S-rGO hybrids. It is seen that BET surface area, pore size, and pore volume of SnO_2/S-rGO hybrids are 173.3 m^2/g, 2.3 nm, and 0.22 cm^3/g, respectively. All these observations suggest that modification of S-rGO with SnO_2 results in formation of porous structure. The presence of porous structure not only provides more specific surface area for contacting with target gas, but also allows for guest molecules infiltrating to the inside of the sensing materials easily, which contribute to offering more active sites to involve the following physicochemical reactions and hence may achieve improved sensing performances.

In order to evaluate sensing performances of SnO_2/S-rGO hybrids, the SnO_2/S-rGO hybrids were selected as sensing materials to fabricate gas sensor for NO_2 sensing at room temperature. Fig. S3 shows the photographs of the SnO_2/S-rGO hybrids-based NO_2 sensor. Fig. 8a shows the response and recovery curve of the sensor based on SnO_2/S-rGO hybrids toward various concentrations of NO_2. It is seen that the resistance of the sensor decreases after introduction of various concentration NO_2, while the resistance recovers back to the initial value after returning the sensor into air, indicating the good response recovery properties of the sensors. Fig. 8b shows the relationship curve between the responses toward NO_2 and corresponding concentrations from 1 ppm to 50 ppm, revealing that the response of sensor increases with increasing the concentrations of NO_2. Additionally, the detection limit of the sensor based on SnO_2/S-rGO hybrids for NO_2 sensing is 450 ppb and the calibration curve of SnO_2/S-rGO sensor as a function of NO_2 concentration at room temperature is shown in Fig. S4.

It has been reported that rGO-based gas sensors exhibit poor response and recovery property, where resistance of the sensor could recover back to the initial value by heating or irradiation by ultraviolet. Although S-rGO exhibits high response toward NO_2, the response time and recovery time are still long (more than several minute) [27]. Fig. 9 shows a typical response and recovery curve of the sensor based on SnO_2/S-rGO hybrids toward 5 ppm NO_2. The response time and recovery time of the sensor in the present work for detection of 5 ppm NO_2 are 40 s and 357 s, which are much shorter than those of S-rGO-based sensors, further indicating the good response and recovery property.

Furthermore, other sensing performances for detection of NO_2 by sensors based on SnO_2/S-rGO hybrids are also examined. Fig. 10 shows the reproducibility of temporal response of SnO_2/S-rGO hybrids exposed to 5 ppm NO_2. Notably, the sensor maintains its initial response amplitude without a clear decrease upon three

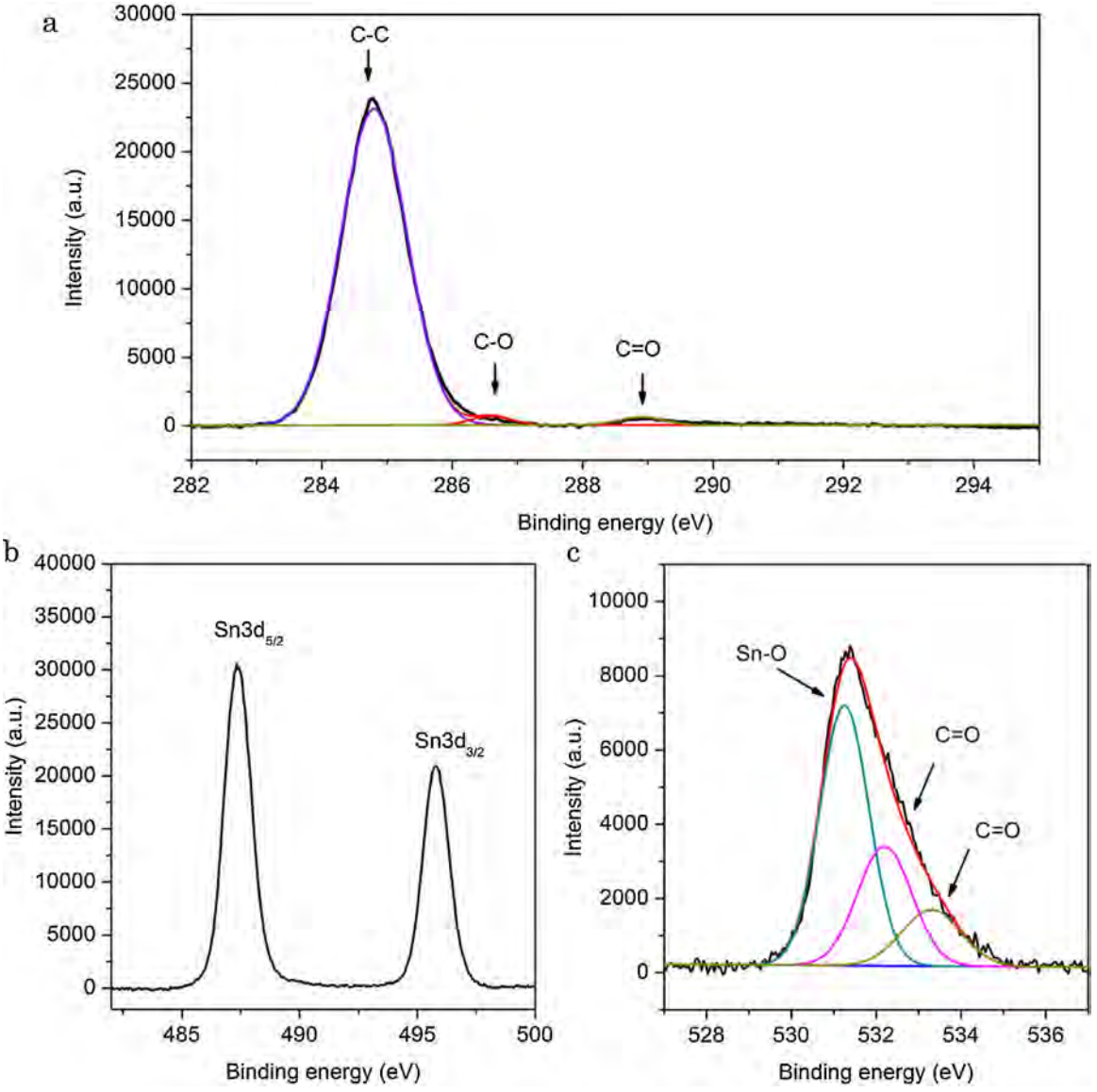

Fig. 3. (a) C1s spectrum, (b) Sn3d spectrum and (c) O1s spectrum of SnO_2/S-rGO hybrids.

successive sensing tests to 5 ppm NO_2, indicating that SnO_2/S-rGO hybrids possess good repeatability. Meanwhile, the selectivity of the sensor based on SnO_2/S-rGO hybrids toward NO_2 sensing is also examined. As shown in Fig. 11, response of the sensor toward 5 ppm NO_2 is 20.31%, which is much higher than that of ammonia (7.25%), Cl_2 (0.53%), CO (1.32%) and C_2H_2 (1.97%), indicating good selectivity of the sensor based on SnO_2/S-rGO hybrids. Additionally, the effect of humidify on the sensing performances is also examined. As shown in Fig. 11. It is seen that the humidity (33% RH and 54% RH) has no effect on gas sensing for SnO_2/S-rGO-based NO_2 sensor. All these observations indicate that SnO_2/S-rGO hybrids are good candidate for development of high performance room temperature NO_2 sensor.

It is well known that a variety of gas sensors based on graphene-based materials have been successfully fabricated. The comparison of the NO_2 sensing performances of sensor based on SnO_2/S-rGO hybrids with previously reported NO_2 sensors using various graphene-based materials is shown in Table 1. Although pure rGO materials, either by chemical reduction of GO [16], or by heat reduction of GO [14], exhibit obvious response toward NO_2 at room temperature, the relatively slow response and recovery rate limits their practical applications. Later, the S-rGO material has been used for detection of NO_2 at room temperature and enhanced gas sensing performances are obtained [27]. Unfortunately, the response time and recovery time are still long more than several minute. Notably, the sensor based on SnO_2/S-rGO hybrids exhibits very short response time and recovery time, providing an effective and simple method for development of NO_2 gas sensor with fast response and recovery rate at room temperature. Furthermore, SnO_2 modified rGO [25] and SnO_2 modified 3D graphene [39] have also been used for detection of NO_2, however, a relatively low temperature (50–55 °C) is still required. Although SnO_2 modified 3D graphene has also been used for fabrication of NO_2 gas sensor operating at room temperature, the sensor exhibits weak response toward NO_2 (the response toward 50 ppm NO_2 is 6.5%) [40]. According to the above discussion, the sensors based on SnO_2/S-rGO hybrids exhibit obvious advantages of low operating temperature, fast response and recovery rate, high sensitivity.

Notably, the novelty of the present work is the introduction of S-rGO into the sensing materials. The improvement of the sensing performances could be attributed to the following reasons. First, the introduction of sulfonate acid into rGO could enhance the dispers-

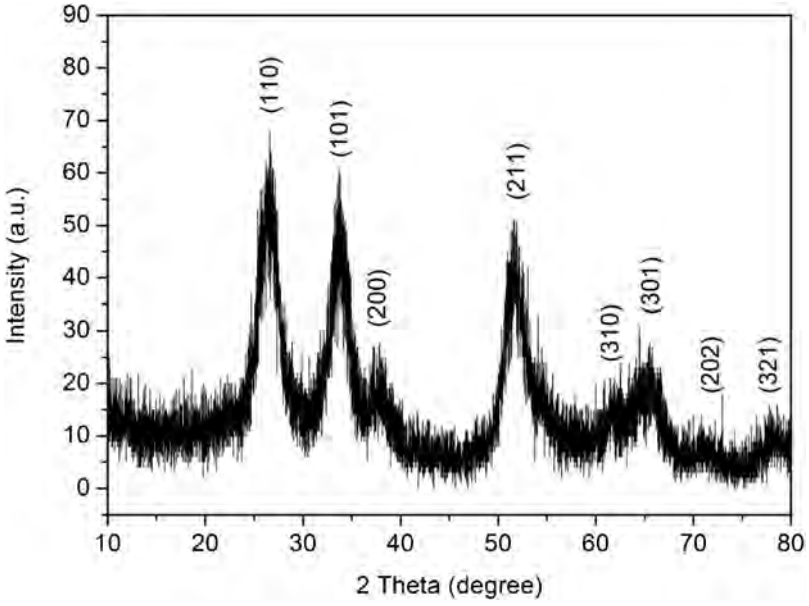

Fig. 4. XRD pattern of SnO_2/S-rGO hybrids.

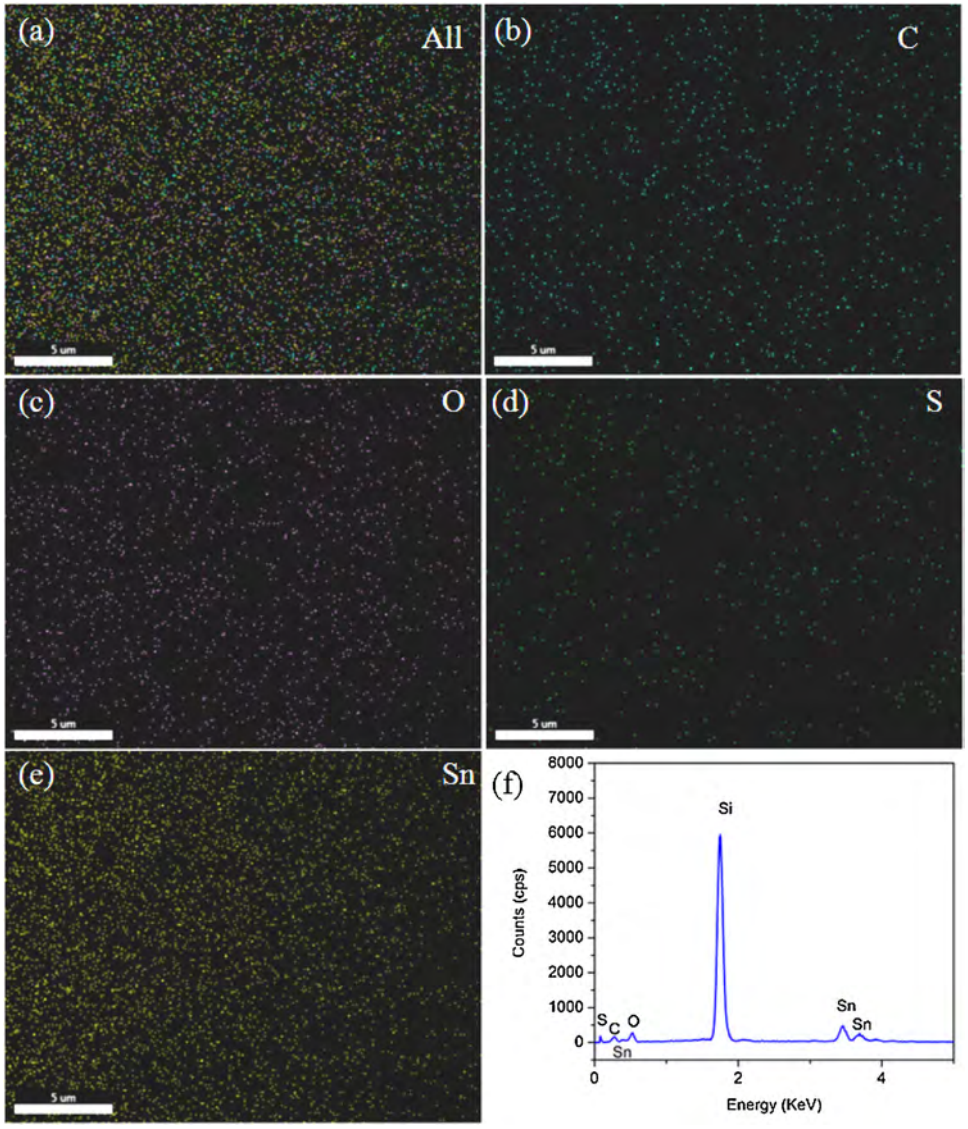

Fig. 5. The EDS mapping for (a) all, (b) C element, (c) O element, (d) S element, (e) Sn element, and (f) corresponding EDS spectrum.

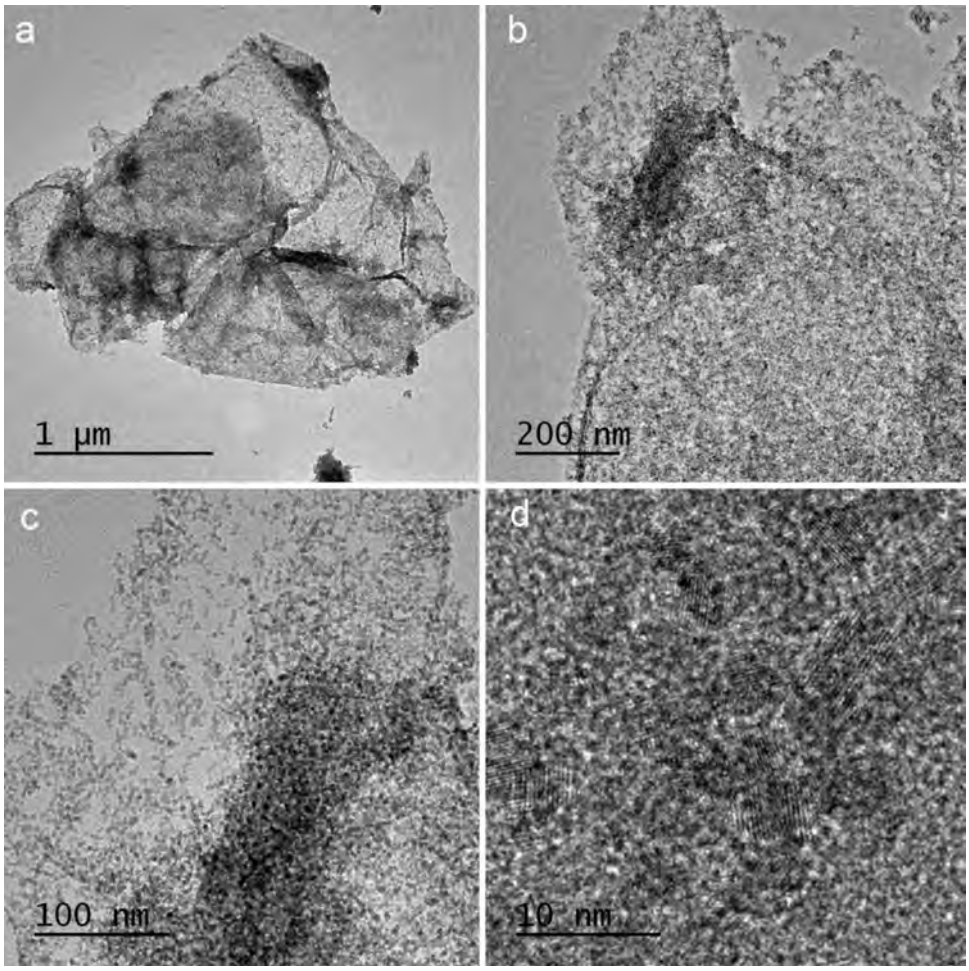

Fig. 6. The TEM images of SnO_2/S-rGO hybrids.

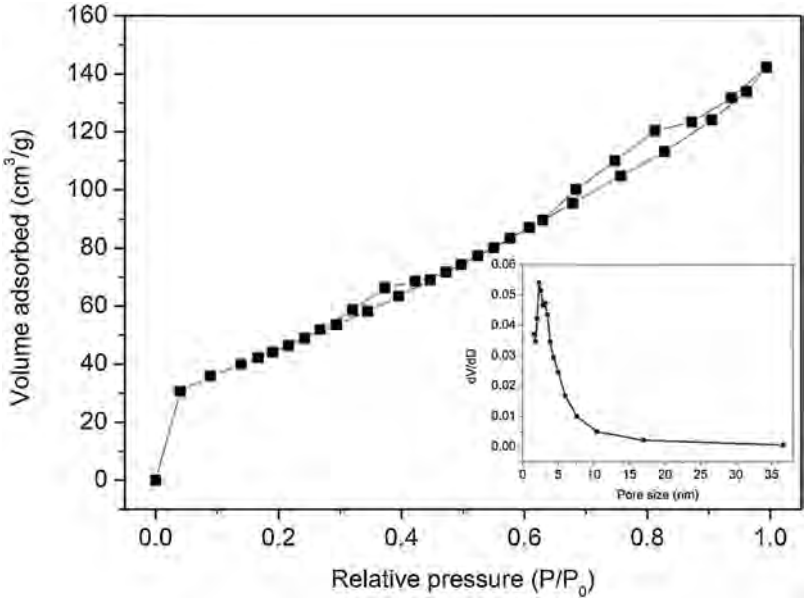

Fig. 7. N_2 sorption isotherms of SnO_2/S-rGO hybrids. Inset shows the corresponding pore size distribution curve.

ing ability of rGO. Second, the S-rGO exhibits better conductivity than that of rGO obtained by hydrothermal method. Most importantly, the enhanced sensing performances are attributed to the formation of p-n junctions between S-rGO and SnO_2, compared to the pure rGO-based NO_2 sensors. Fig. 12 shows the scheme to illustrate the electrons transfer progress between S-rGO and SnO_2 during the NO_2 sensing, which is similar with our previous reported NO_2 sensors based on rGO and metal oxides hybrids [25,26,41].

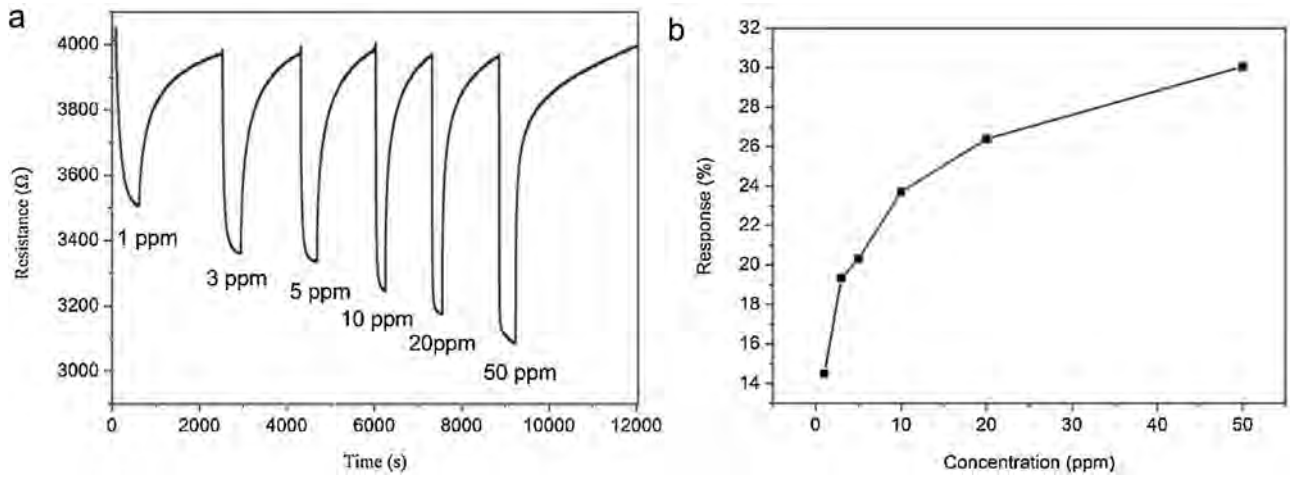

Fig. 8. (a) Dynamic sensing responses of SnO_2/S-rGO sensors upon exposure to NO_2 gas with concentrations varying from 1 to 50 ppm, and (b) the corresponding response variations of SnO_2/S-rGO sensors as a function of NO_2 concentrations.

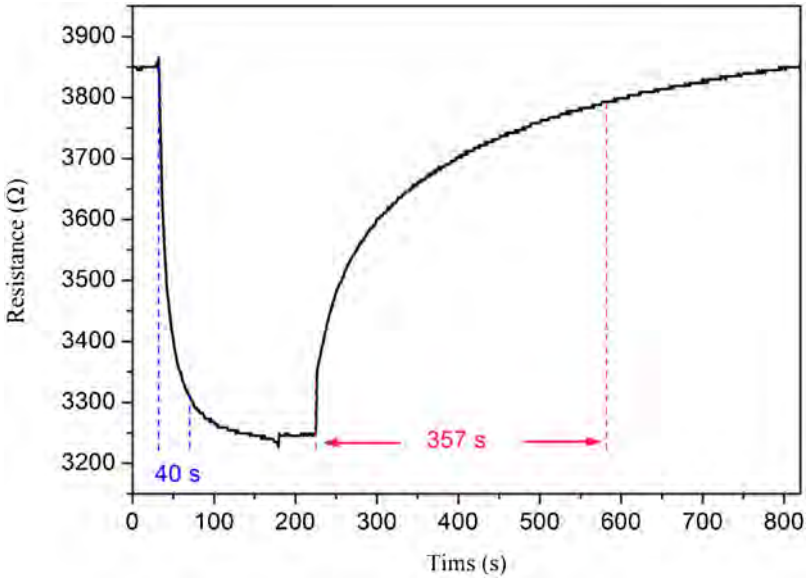

Fig. 9. The response and recovery curve of the sensor based on SnO_2/S-rGO hybrids toward 5 ppm NO_2 at room temperature.

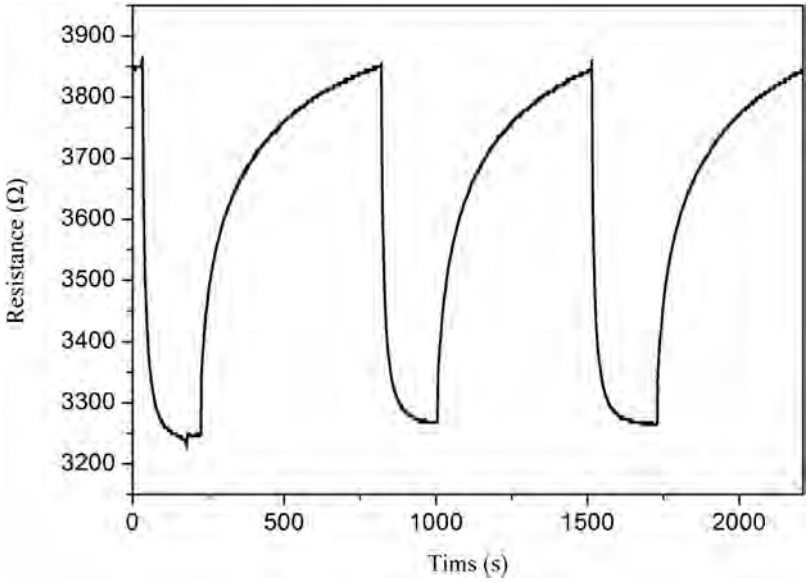

Fig. 10. The reproducibility of temporal response of SnO_2/S-rGO hybrids exposed to 5 ppm NO_2 at room temperature.

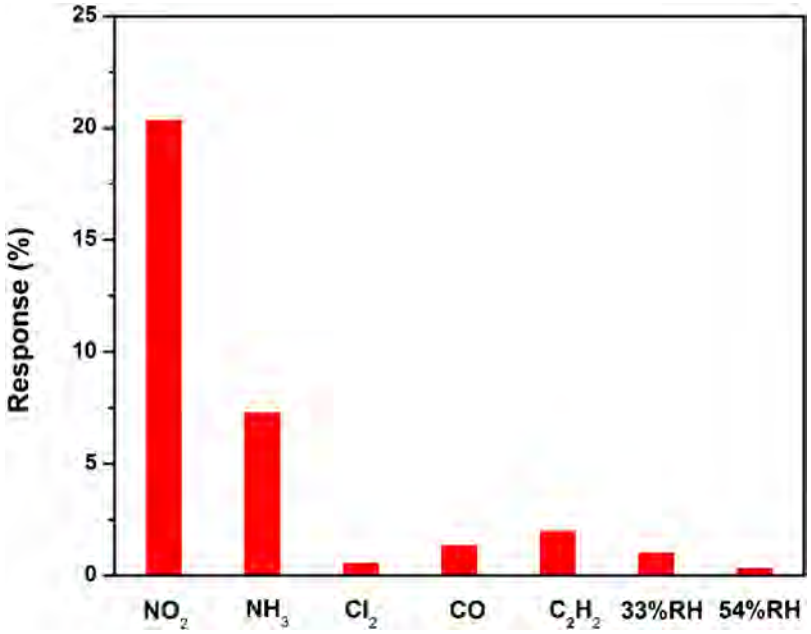

Fig. 11. Comparison of responses of SnO_2/S-rGO hybrids to various gases at room temperature.

Table 1
Comparison of sensing performances of our proposed NO_2 sensor with other published NO_2 sensors based on rGO-based materials.

Sensing materials	Method	Operating temperature	Concentration	Sensing performances		Refs.
				Response	Response time/recovery time	
rGO[b]	Chemical reduction	RT	25–100 ppm	141 (100 ppm)	Few min/few min	[12]
rGO[c]	Heat reduction	RT	10–100 ppm	9.15 (100 ppm)	Few min/few min	[14]
S-rGO	Wet chemical	RT	5–45 ppm	24.7 (50 ppm)	Few min/few min	[25]
SnO_2/rGO	hydrothermal	50 °C	0.5–500 ppm	3.31 (5 ppm)	135 s/200 s	[23]
3D graphene/SnO_2	hydrothermal	55 °C	14–140 ppm	1.115 (100 ppm)	Few min/few min	[39]
3D graphene/SnO_2	hydrothermal	RT	10–200 ppm	1.065 (50 ppm)	190 s/224 s	[40]
SnO_2/S-rGO	Wet chemical	RT	1–50 ppm	1.203 (5 ppm)	40 s/357 s	This work

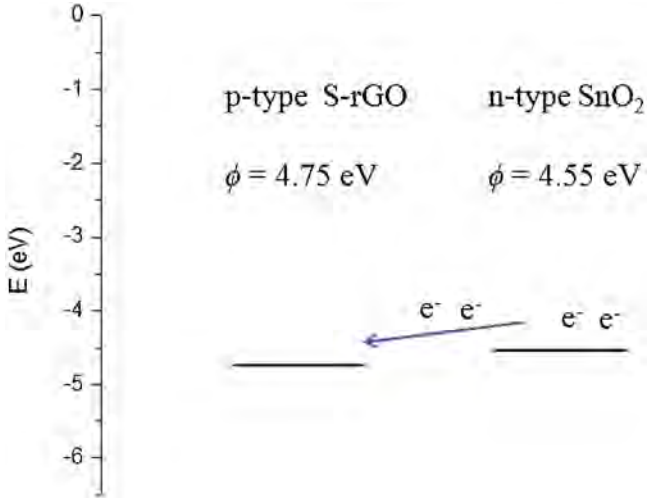

Fig. 12. The scheme to illustrate the electrons transfer progress between S-rGO and SnO_2 during the NO_2 sensing.

4. Conclusion

In summary, a new room temperature NO_2 sensor has been successfully fabricated by using SnO_2/S-rGO hybrids as sensing materials, where SnO_2/S-rGO hybrids have been prepared by hydrothermal synthesis method. The gas sensing results indicate that the introduction of SnO_2 nanoparticles onto the surface of S-rGO significantly enhanced the NO_2 sensing performances at room temperature. Our present study is of importance because it provides a new sensing material for fabrication of high-performance room temperature NO_2 sensors.

Acknowledgments

This research work was financially supported by the National Natural Science Foundation of China (Grant No. 51202085), Program for Chang Jiang Scholars and Innovative Research Team in University (No. IRT3018) and the Open Project from State Key Laboratory of Transducer Technology (Grant No. SKT1402).

Appendix A. Supplementary data

Supplementary data associated with this article can be found, in the online version, at http://dx.doi.org/10.1016/j.snb.2016.01.023.

References

[1] K.S. Novoselov, A.K. Geim, S.V. Morozov, D. Jiang, Y. Zhang, S.V. Dubonos, I.V. Grigorieva, A.A. Firsov, Electric field effect in atomically thin carbon films, Science 306 (2004) 666–669.
[2] S. Stankovich, D.A. Dikin, R.D. Piner, K.A. Kohlhaas, A. Kleinhammes, Y. Jia, Y. Wu, S.T. Nguyen, R.S. Ruoff, Synthesis of graphene-based nanosheets via chemical reduction of exfoliated graphite oxide, Carbon 45 (2007) 1558–1565.
[3] X. Huang, X. Qi, F. Boey, H. Zhang, Graphene-based composites, Chem. Soc. Rev. 41 (2012) 666–686.

[4] Z.-S. Wu, W. Ren, L. Wen, L. Gao, J. Zhao, Z. Chen, G. Zhou, F. Li, H.-M. Cheng, Graphene anchored with Co_3O_4 nanoparticles as anode of lithium ion batteries with enhanced reversible capacity and cyclic performance, ACS Nano 4 (2010) 3187–3194.
[5] W. Yuan, G. Shi, Graphene-based gas sensors, J. Mater. Chem. A 1 (2013) 10078–10091.
[6] S. Singkammo, A. Wisitsoraat, C. Sriprachuabwong, A. Tuantranont, S. Phanichphant, C. Liewhiran, Electrolytically exfoliated graphene-loaded flame-made Ni-doped SnO_2 composite film for acetone sensing, ACS Appl. Mater. Interfaces 7 (2015) 3077–3092.
[7] K. Inyawilert, A. Wisitsoraat, C. Sriprachaubwong, A. Tuantranont, S. Phanichphant, C. Liewhiran, Rapid ethanol sensor based on electrolytically-exfoliated graphene-loaded flame-made in-doped SnO_2 composite film, Sens. Actuators B 209 (2015) 40–55.
[8] Z. Zhang, R. Zou, G. Song, L. Yu, Z. Chen, J. Hu, Highly aligned SnO_2 nanorods on graphene sheets for gas sensors, J. Mater. Chem. 21 (2011) 17360–17365.
[9] L. Yin, D. Chen, X. Cui, L. Ge, J. Yang, L. Yu, B. Zhang, R. Zhang, G. Shao, Normal-pressure microwave rapid synthesis of hierarchical SnO_2@rGO nanostructures with super high surface areas as high-quality gas-sensing and electrochemical active materials, Nanoscale 6 (2014) 13690–136700.
[10] S.-J. Choi, B.-H. Jang, S.-J. Lee, B.K. Min, A. Rothschild, I.-D. Kim, Selective detection of acetone and hydrogen sulfide for the diagnosis of diabetes and halitosis using SnO_2 nanofibers functionalized with reduced graphene oxide nanosheets, ACS Appl. Mater. Interfaces 6 (2014) 2588–2597.
[11] X. An, J.C. Yu, Y. Wang, Y. Hu, X. Yu, G. Zhang, WO3 nanorods/graphene nanocomposites for high-efficiency visible-light-driven photocatalysis and NO_2 gas sensing, J. Mater. Chem. 22 (2012) 8525–8531.
[12] F. Schedin, A.K. Geim, S.V. Morozov, E.W. Hill, P. Blake, M.I. Katsnelson, K.S. Novoselov, Detection of individual gas molecules adsorbed on graphene, Nat. Mater. 6 (2007) 652–655.
[13] F. Yavari, Z. Chen, A.V. Thomas, W. Ren, H.-M. Cheng, N. Nikil, High sensitivity gas detection using a macroscopic three-demensional graphene foam network, Sci. Rep. 1 (2011) 166.
[14] G. Lu, L.E. Ocola, J. Chen, Reduced graphene oxide for room-temperature gas sensors, Nanotechnology 20 (2009) 445502.
[15] J. Wang, Y. Kwar, I. Lee, S. Maeng, G.-H. Kim, Highly responsive hydrogen gas sensing by partially reduced graphite oxide thin films at room temperature, Carbon 50 (2012) 4061–4067.
[16] G. Lu, S. Park, K. Yu, R.S. Ruoff, L.E. Ocola, D. Rosenmann, J. Chen, Toward practical gas sensing with highly reduced graphene oxide: a new signal processing method to circumvent run-to-run and device-to-device variations, ACS Nano 5 (2015) 1154–1164.
[17] D.-T. Phan, G.-S. Chung, Effect of Pd nanocube size of Pd nanocube hybrid on hydrogen sensing properties, Sens. Actuators B 204 (2014) 437–444.
[18] Y. Yang, S. Li, W. Yang, W. Yuan, J. Xu, Y. Jiang, In situ polymerization deposition of porous conducting polymer on reduced graphene oxide for gas sensor, ACS Appl. Mater. Interface 6 (2014) 13807–13814.
[19] P.A. Russo, N. Donato, S.G. Leonardi, S. Baek, D.E. Conte, G. Neri, N. Pinna, Room-temperature hydrogen sensing with heteronanostructures based on reduced graphene oxide and tin oxide, Angew. Chem. Int. Ed. 51 (2012) 11053–11057.
[20] Q. Li, Y. Li, M. Yang, Tin oxide/graphene composite fabricated via a hydrothermal method for gas sensors working at room temperature, Sens. Actuators B 173 (2012) 139–147.
[21] Y. Yang, C. Tian, J. Wang, L. Sun, K. Shi, W. Zhou, H. Fu, Facile synthesis of novel 3D nanoflower-like CuxO/multilayer graphene composites for room temperature NOx gas sensor application, Nanoscale 6 (2014) 7369–7378.
[22] N. Chen, X. Li, X. Wang, J. Yu, J. Wang, Z. Tang, S.A. Akbar, Enhanced room temperature sensing of Co_3O_4-intercalated reduced graphene oxide based gas sensors, Sens. Actuators B 188 (2013) 902–908.
[23] G. Singh, A. Choudhary, D. Haranath, A.G. Joshi, N. Singh, S. Singh, R. Pasricha, ZnO decorated luminescent graphene as a potential gas sensor at room temperature, Carbon 50 (2012) 385–394.
[24] S. Liu, B. Yu, H. Zhang, T. Fei, T. Zhang, Enhancing NO_2 gas sensing performances at room temperature based on reduced graphene oxide–ZnO nanoparticles hybrids, Sens. Actuators B 202 (2014) 272–278.
[25] H. Zhang, J. Feng, T. Fei, S. Liu, T. Zhang, SnO_2 nanoparticles-reduced graphene oxide nanocomposites for NO_2 sensing at low operating temperature, Sens. Actuators B 190 (2014) 472–478.
[26] S. Liu, Z. Wang, Y. Zhang, C. Zhang, T. Zhang, High performance room temperature NO_2 sensors based on reduced graphene oxide-multiwalled carbon nanotubes-tin oxide nanoparticles hybrids, Sens. Actuators B 211 (2015) 318–324.
[27] W. Yuan, A. Liu, L. Huang, C. Li, G. Shi, High-performance NO_2 sensors based on chemically modified graphene, Adv. Mater. 25 (2013) 766–771.
[28] W.S. Hummers Jr., R.E. Offeman, Preparation of graphite oxide, J. Am. Chem. Soc. 80 (1958) 1339.
[29] Y. Si, E.T. Samulski, Synthesis of water soluble graphene, Nano Lett. 8 (2008) 1679–1682.
[30] S. Deng, V. Tjoa, H.M. Fan, H.R. Tan, D.C. Sayle, M. Plivo, S. Mhaisalkar, J. Wei, C.H. Sow, Reduced graphene oxide conjugated Cu_2O nanowire mesocrystals for high-performance NO_2 gas sensor, J. Am. Chem. Soc. 134 (2012) 4905–4917.
[31] S. Mao, S. Cui, G. Lu, K. Yu, Z. Wen, J. Chen, Tuning gas-sensing properties of reduced graphene oxide using tin oxide nanocrystals, J. Mater. Chem. 22 (2012) 11009–11013.
[32] B. Cai, X. Lv, S. Gan, M. Zhou, W. Ma, T. Wu, F. Li, D. Han, L. Niu, Advanced visible-light-driven photocatalyst upon the incorporation of sulfonated graphene, Nanoscale 5 (2013) 1910–1916.
[33] L. Huang, Z. Wang, J. Zhang, J. Pu, Y. Lin, S. Xu, L. Shen, Q. Chen, W. Shi, Fully printed, rapid-response sensors based on chemically modified graphene for detecting NO_2 at room temperature, ACS Appl. Mater. Interfaces 6 (2014) 7426–7433.
[34] D. Li, M.B. Müller, S. Gilje, R.B. Kaner, G.G. Wallace, Processable aqueous dispersions of graphene nanosheets, Nat. Nanotechnol. 3 (2008) 101–105.
[35] S. Liu, J. Tian, L. Wang, X. Sun, A method for the production of reduced graphene oxide using benzylamine as a reducing and stabilizing agent and its subsequent decoration with Ag nanoparticles for enzymeless hydrogen peroxide detection, Carbon 49 (2011) 3158–3164.
[36] X.W. Lou, Y. Wang, C. Yuan, J.Y. Lee, L.A. Archer, Template-free synthesis of SnO_2 hollow nanostructures with high lithium storage capacity, Adv. Mater. 18 (2006) 2325–2329.
[37] L. Wang, S. Wang, Y. Wang, H. Zhang, Y. Kang, W. Huang, Synthesis of hierarchical SnO_2 nanostructures assembled with nanosheets and their improved gas sensing properties, Sens. Actuators B 188 (2013) 85–93.
[38] S. Liu, Y. Zhang, B. Yu, Z. Wang, H. Zhao, N. Zhou, T. Zhang, Solvent-free infiltration method to prepare mesoporous SnO_2 templated by SiO_2 nanoparticles for ethanol sensing, Sens. Actuators B 210 (2015) 700–705.
[39] L. Li, S. He, M. Liu, C. Zhang, W. Chen, Three-dimensional mesoporous graphene aerogel-supported SnO_2 nanocrystals for high-performance NO_2 gas sensing at low temperature, Anal. Chem. 87 (2015) 1638–1645.
[40] X. Liu, J. Cui, J. Sun, X. Zhang, 3D graphene aerogel-supported SnO_2 nanoparticles for efficient detection of NO_2, RSC Adv. 4 (2014) 22601–22605.
[41] Z. Wang, Y. Zhang, S. Liu, T. Zhang, Preparation of Ag nanoparticles–SnO_2 nanoparticles-reduced graphene oxide hybrids and their application for detection of NO_2 at room temperature, Sens. Actuators B 222 (2016) 893–903.

Biographies

Sen Liu received his B.S. degree in 2005 in Chemistry and Ph.D. degree in 2010 in Inorganic Chemistry from Jilin University. Now he is an associate professor in Jilin University and his current research is focused on the carbon-based functional materials and chemical sensors.

Ziying Wang received her B.S. degree from the College of Electronics Science and Engineering, Jilin University, China in 2013. During BS course, She studied in Tomsk and received her B.S. degree from the College of Institute of Non-Destructive Testing, Tomsk Polytechnic University, Russia in 2013. She entered the M.S. course in 2013. Now her research focuses on preparation of gas sensors and flexible strain sensors.

Yong Zhang received his B.S. degree from the College of Science, Changchun University of Science and Technology, China in 2011. He received his M.S. degree from the College of Science, Changchun University of Science and Technology, China in 2014. During M.S. course, he took part in the joint training program for two years in Changchun Institute of Applied Chemistry, Chinese Academy of Sciences. He entered the D.S. course in 2014, majoring in microelectronics and solid-state electronics. His research focuses on the preparation of electrochemical sensor based on nano-micron functional materials.

Jiacheng Li received his BS degree from the College of Electronics Science and Engineering, Jilin University, China in 2015. His research interests include sensing functional materials for gas sensors.

Tong Zhang completed her M.S. degree in semiconductor materials in 1992 and her Ph.D. in the field of microelectronics and solid-state electronics in 2001 from Jilin University. She was appointed as a full-time professor in the College of Electronics Science and Engineering, Jilin University in 2001. Her research interests are sensing functional materials, gas sensors, humidity sensors and electrochemical sensors.